

## Supplementary Material

### Photophysical and electrochemical properties of two trans-A<sub>2</sub>B-corroles: Differences between phenyl or pyrenyl groups *meso*-10 position

Thiago V. Acunha,<sup>a</sup> Henrique F.V. Victória,<sup>b</sup> Klaus Krambrock,<sup>b</sup> Amanda C. Marques,<sup>c</sup> Luiz Antônio S. Costa<sup>c</sup> and Bernardo A. Iglesias<sup>a\*</sup>

<sup>a</sup>*Laboratório de Bioinorgânica e Materiais Porfirínicos, Departamento de Química, Universidade Federal de Santa Maria - UFSM, Av. Roraima 1000, 97105-900 Santa Maria, RS, Brazil.*

<sup>b</sup>*Instituto de Ciências Exatas, Departamento de Física, Universidade Federal de Minas Gerais, Av. Antônio Carlos 6627, 31270-901, Belo Horizonte, MG, Brazil.*

<sup>c</sup>*NEQC – Núcleo de Estudos em Química Computacional, Departamento de Química, Universidade Federal de Juiz de Fora - UFJF, Campus Universitário s/n, 36036-900, Juiz de Fora, MG, Brazil.*

## Synthetic methodology

### Synthesis of 5,15-bis(pentafluorophenyl)-10-(phenyl)corrole **1a** and 5,15-bis(pentafluorophenyl)-10-(1-pyrenyl)corrole **1b**

The same synthetic methodology was used for the synthesis of the two mono-substituted corroles<sup>1,2</sup>. C<sub>6</sub>F<sub>5</sub>-DPM (0.094 g; 0.30 mmol) and the respective aldehyde (16 µL; 0.15 mmol for PhCHO and 0.034 g; 0.15 mmol for PyrCHO) were dissolved in 50 mL MeOH. Subsequently, a solution of HCl<sub>aq</sub> (37%; 2.0 mL) in H<sub>2</sub>O (50 mL) was added and the reaction was stirred at room temperature for 1.0 h. The mixture was extracted with CHCl<sub>3</sub>, and the organic layer was washed twice with water, dried (Na<sub>2</sub>SO<sub>4</sub>), filtered, and diluted to 250 mL with CH<sub>2</sub>Cl<sub>2</sub>. A solution of *p*-chloranil (0.111 g; 0.45 mmol) in dichloromethane was added, and the mixture was stirred for 24 h. The reaction mixture was concentrated to half of this volume and it was purified first on a silica-gel chromatography column (CH<sub>2</sub>Cl<sub>2</sub>/hexane, 1:2, v/v). Then, the resulting residue was purified again by preparative silica-gel TLC plates using the same mixture, to obtain pure dark purple corroles **1a** and **1b**, respectively.

**Spectroscopic data for corrole **1a**:** Yield 0.019 g; 0.027 mmol (18%). M.p. > 300°C (decomp.). <sup>1</sup>H NMR (600.13 MHz, CDCl<sub>3</sub>): δ = 7.77 (m, 3H; H<sub>a</sub>), 8.19 (m, 2H; H<sub>b</sub>), 8.57 (bs, 2H; H<sub>3,17</sub>), 8.70 (s, 4H; H<sub>β</sub>), 9.13 (d, 2H, J = 6.0 Hz; H<sub>2,18</sub>). <sup>19</sup>F RMN (564.68 MHz, CDCl<sub>3</sub>): -161.78 (m, 4F; F<sub>meta</sub>), -152.85 (bs, 2F; F<sub>para</sub>), -137.84 (m, 4F; F<sub>ortho</sub>). FT-IR (KBr pellets, cm<sup>-1</sup>): 3358 (v<sub>N—H</sub>), 2923 (v<sub>C=C</sub>), 1519 (v<sub>C=N</sub>), 987 (v<sub>C—N</sub>), 759 (δ<sub>C—H</sub>). Anal. Calcd for C<sub>37</sub>H<sub>16</sub>N<sub>4</sub>F<sub>10</sub> (%): C, 62.90; H, 2.28; N, 7.93. Found (%): C, 62.98; H, 2.29; N, 7.97. HRMS-APCI-(+) [M+H]<sup>+</sup>: m/z = 707.1284 (calcd for C<sub>37</sub>H<sub>17</sub>N<sub>4</sub>F<sub>10</sub>: 707.1288).

**Spectroscopic data for corrole **1b**:** Yield 0.015 g; 0.018 mmol (12%). M.p.> 300°C (decomp.). <sup>1</sup>H NMR (600.13 MHz, CDCl<sub>3</sub>): δ = 7.48 (d, 1H, J = 12.0 Hz; H<sub>d</sub>), 7.73 (d, 1H, J = 12.0 Hz; H<sub>e</sub>), 8.08 (m, 1H; H<sub>c</sub>), 8.13 (d, 1H, J = 12.0 Hz; H<sub>f</sub>), 8.35 (dd, 4H, J<sup>1</sup> = 12.0 Hz e J<sup>2</sup> = 6.0 Hz; H<sub>i</sub>, H<sub>b</sub> and H<sub>3,17</sub>), 8.40 (d, 1H, J = 6.0 Hz; H<sub>g</sub>), 8.53 (d, 1H, J = 6.0 Hz; H<sub>a</sub>), 8.59 (s, 4H; H<sub>β</sub>), 8.73 (d, 1H, J = 12.0 Hz; H<sub>j</sub>), 9.15 (d, 2H, J = 6.0 Hz; H<sub>2,18</sub>). <sup>19</sup>F RMN (564.68 MHz, CDCl<sub>3</sub>): -165.78 (m, 4F; F<sub>meta</sub>), -156.86 (bs, 2F; F<sub>para</sub>), -141.85 (m, 4F; F<sub>ortho</sub>). FT-IR (KBr pellets, cm<sup>-1</sup>): 3250 (v<sub>N—H</sub>), 2924 (v<sub>C=C</sub>), 2853 (v<sub>C=C</sub>), 1522 (v<sub>C=N</sub>), 988 (v<sub>C—N</sub>), 801 (δ<sub>C—H</sub>). Anal. Calcd for C<sub>47</sub>H<sub>20</sub>N<sub>4</sub>F<sub>10</sub> (%): C, 67.96; H, 2.43; N, 6.74. Found (%): C, 68.03; H, 2.46; N, 6.88. HRMS-APCI-(+) [M+H]<sup>+</sup>: m/z = 831.1601 (calcd for C<sub>47</sub>H<sub>21</sub>N<sub>4</sub>F<sub>10</sub>: 831.1601).

## Tables

**Table S1.** Elemental analysis (CHN%) of corroles **1a** and **1b**.

	Corrole <b>1a</b>	Corrole <b>1b</b>
%C <sub>exp</sub> ; %C <sub>calcd</sub>	62.98; 62.90	68.03; 67.96
%H <sub>exp</sub> ; %H <sub>calcd</sub>	2.29; 2.28	2.46; 2.43
%N <sub>exp</sub> ; %N <sub>calcd</sub>	7.97; 7.93	6.88; 6.74
<b>Molecular formula</b>	C <sub>37</sub> H <sub>16</sub> F <sub>10</sub> N <sub>4</sub>	C <sub>47</sub> H <sub>20</sub> F <sub>10</sub> N <sub>4</sub>

**Table S2.** Main geometric parameters of corroles **1a** and **1b**. Bond lengths are given in angstroms (Å).

Bond lengths	Corrole <b>1a</b>		Corrole <b>1b</b>	
	Singlet ( <sup>1</sup> S <sub>0</sub> )	Triplet ( <sup>3</sup> S <sub>0</sub> )	Singlet ( <sup>1</sup> S <sub>0</sub> )	Triplet ( <sup>3</sup> S <sub>0</sub> )
<b>H35–H36</b>	2.130	2.153	2.111	2.164
<b>H35–H37</b>	2.067	2.250	2.077	2.206
<b>N9–N16</b>	2.636	2.648	2.697	2.644
<b>N9–N24</b>	3.903	3.935	3.896	3.929
<b>N9–N31</b>	2.639	2.679	2.640	2.678
<b>N9–H35</b>	1.029	1.025	1.028	1.025
<b>N9–C8</b>	1.367	1.372	1.367	1.372
<b>N9–C4</b>	1.369	1.364	1.369	1.364
<b>N9–C15</b>	2.838	2.862	2.839	2.861
<b>N16–C15</b>	1.383	1.365	1.382	1.363
<b>N16–C11</b>	1.369	1.386	1.368	1.387
<b>N16–C23</b>	3.053	3.059	3.053	3.067
<b>N24–C23</b>	1.384	1.384	1.384	1.384
<b>N24–C32</b>	1.391	1.384	1.392	1.384
<b>N24–C28</b>	2.996	3.014	2.992	3.008
<b>N31–C28</b>	1.379	1.384	1.380	1.384
<b>N31–C30</b>	1.383	1.379	1.383	1.380
<b>N31–N24</b>	2.765	2.835	2.760	2.825
<b>C8–C15</b>	2.485	2.508	2.485	2.508
<b>C11–C23</b>	2.521	2.543	2.520	2.542
<b>C32–C28</b>	2.484	2.510	2.484	2.513
<b>C4–C30</b>	1.419	1.456	1.420	1.456

**Table S3.** Bader's atomic point charge. Last column presents the percentual difference between the absolute values.

Corrole 1b			
Atom / State	S	T	Percentual Diff.
<b>N9</b>	-1.1485	-1.1466	0.16
<b>N16</b>	-1.0428	-1.0066	3.47
<b>N24</b>	-1.1038	-1.0887	1.37
<b>N31</b>	-1.0913	-1.1048	1.22
<b>H35</b>	+0.4901	+0.4878	0.47
<b>H36</b>	+0.4361	+0.4384	0.52
<b>H37</b>	+0.4452	+0.4466	0.31
<b>C4</b>	+0.3872	+0.3926	1.37
<b>C11</b>	+0.3789	+0.3408	10.0
<b>C17</b>	-0.0102	+0.0172	40.7
<b>C23</b>	+0.3623	+0.3423	5.52
<b>C30</b>	+0.3537	+0.3556	0.53
<b>C<sub>Pyr/Ph</sub></b>	-0.0098	-0.0150	34.7

## Figures

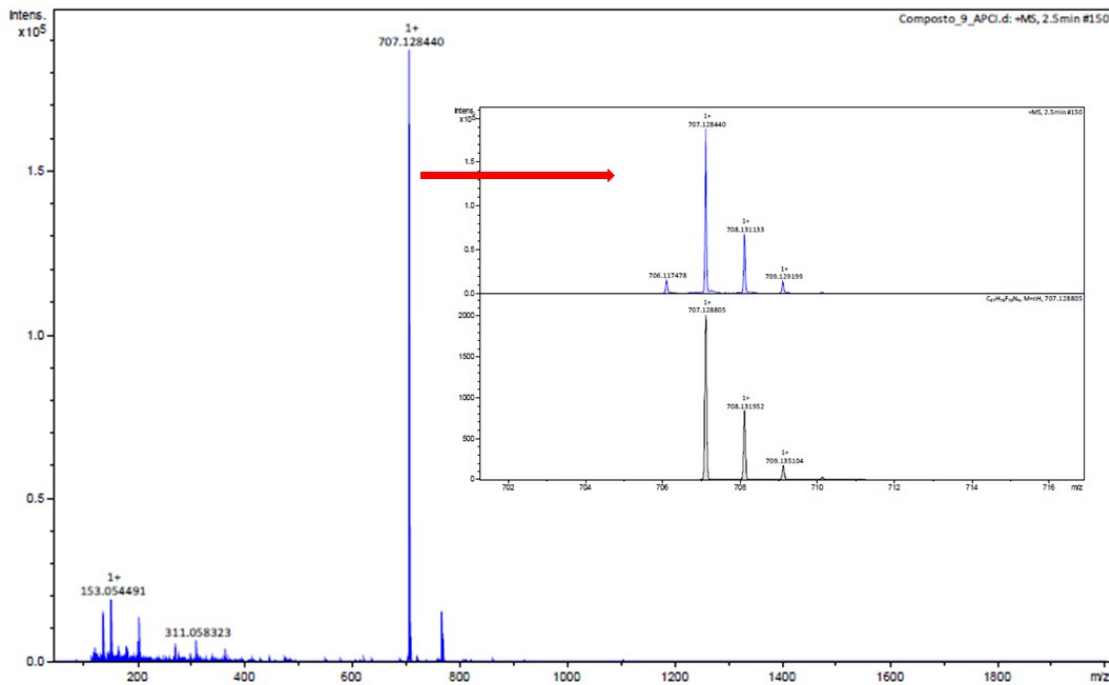


**Figure S1.** HRMS-APCI mass spectra analysis of corrole **1a**, in the positive mode.

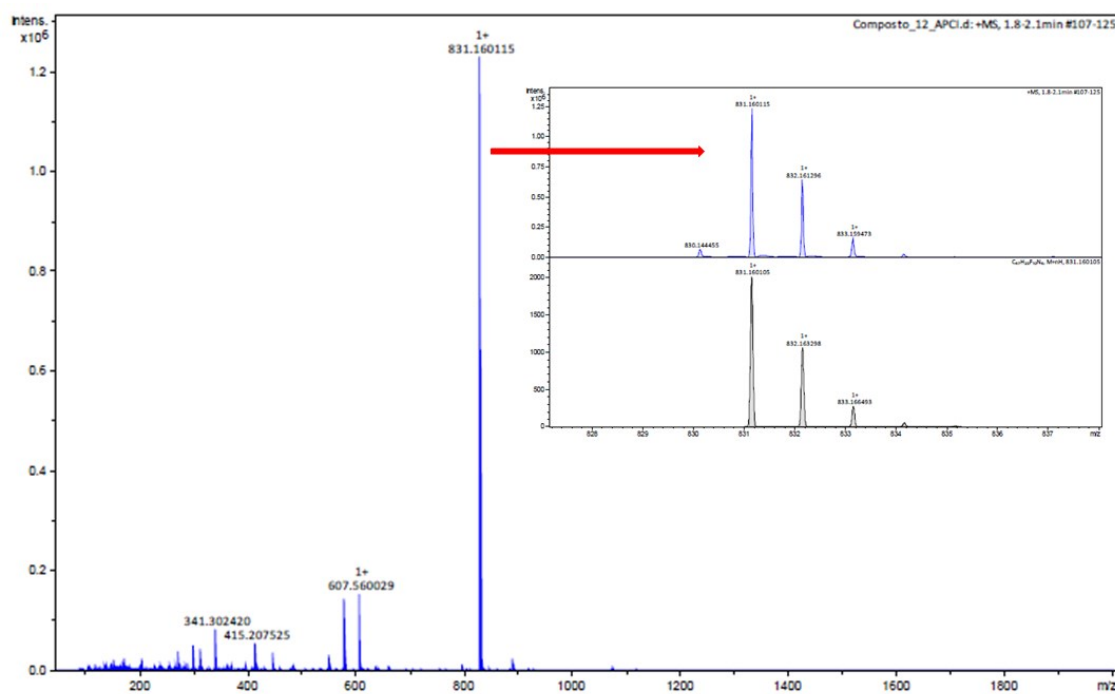


**Figure S2.** HRMS-APCI mass spectra analysis of corrole **1b**, in the positive mode.

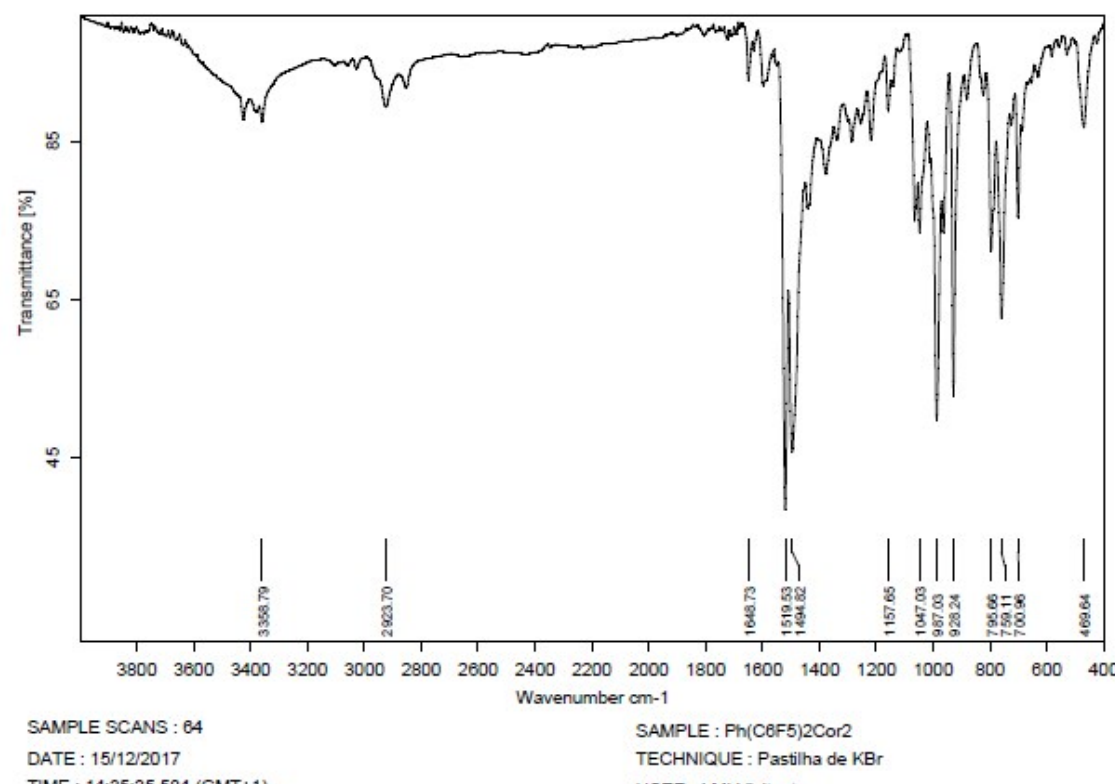


**Figure S3.** FTIR vibrational spectra analysis of corrole **1a**, in KBr pellets, at 4000 to 400  $\text{cm}^{-1}$ .

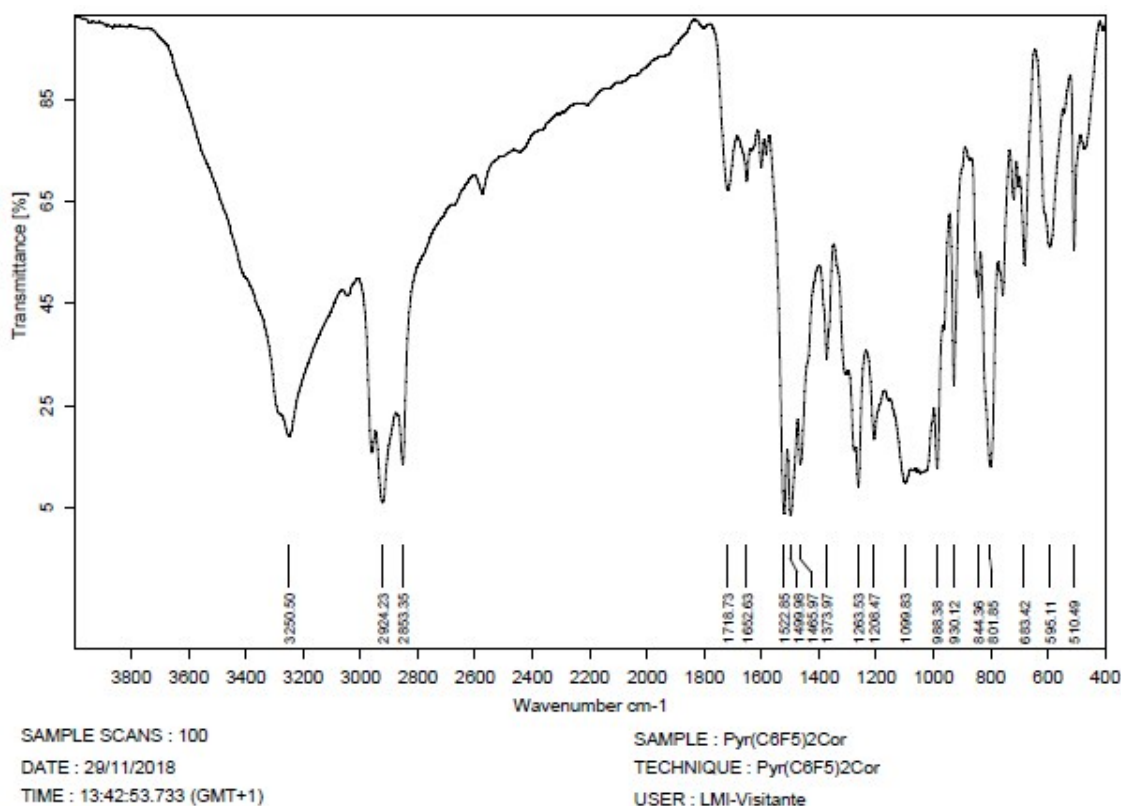


**Figure S4.** FTIR vibrational spectra analysis of corrole **1b**, in KBr pellets, at 4000 to 400  $\text{cm}^{-1}$ .

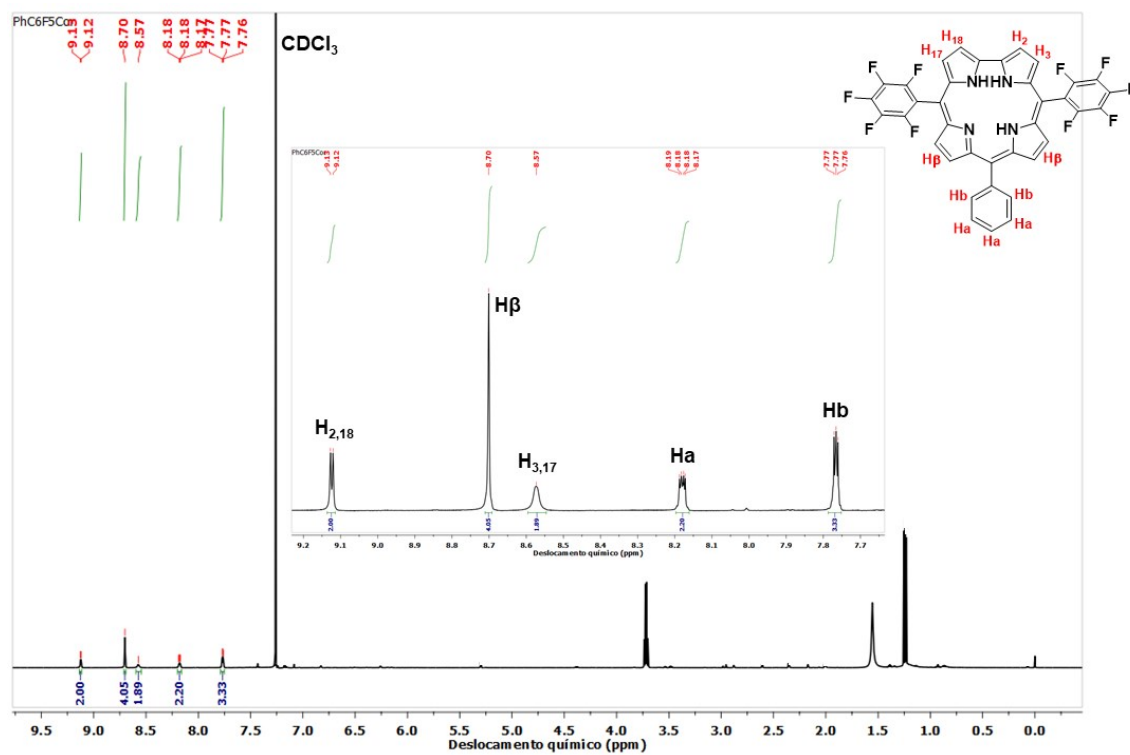


**Figure S5.**  $^1\text{H}$ -NMR spectra of corrole **1a**, in  $\text{CDCl}_3$ .

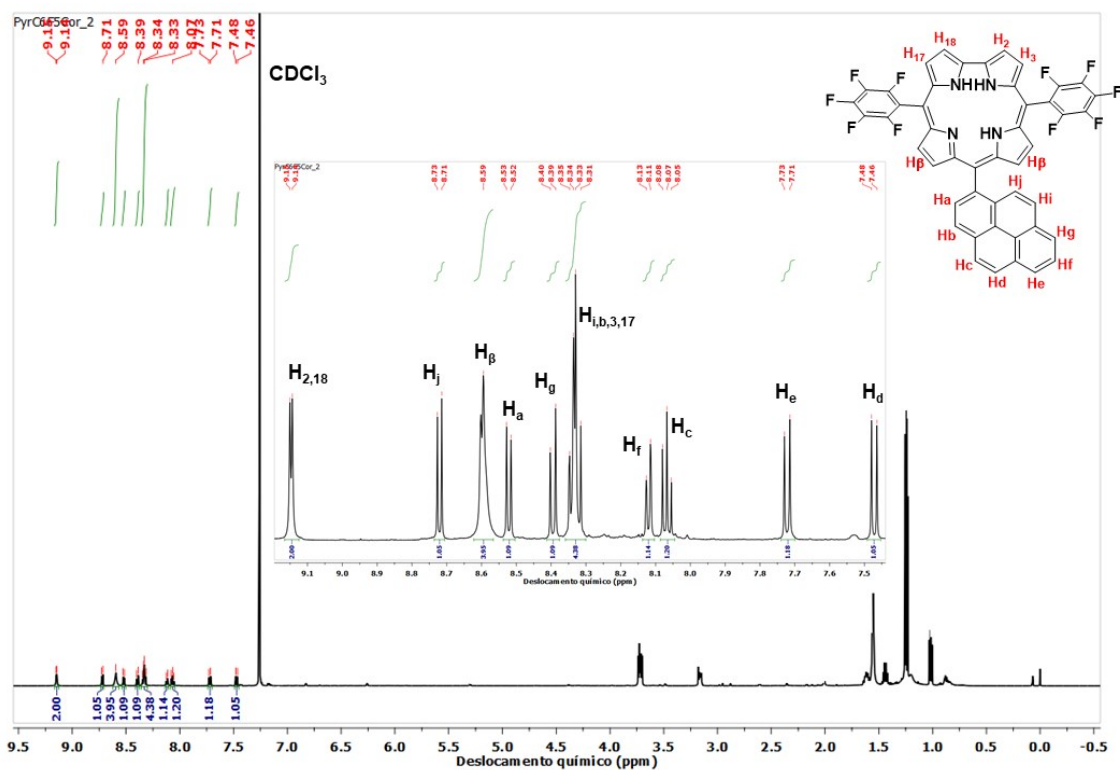


**Figure S6.**  $^1\text{H}$ -NMR spectra of corrole **1b**, in  $\text{CDCl}_3$ .

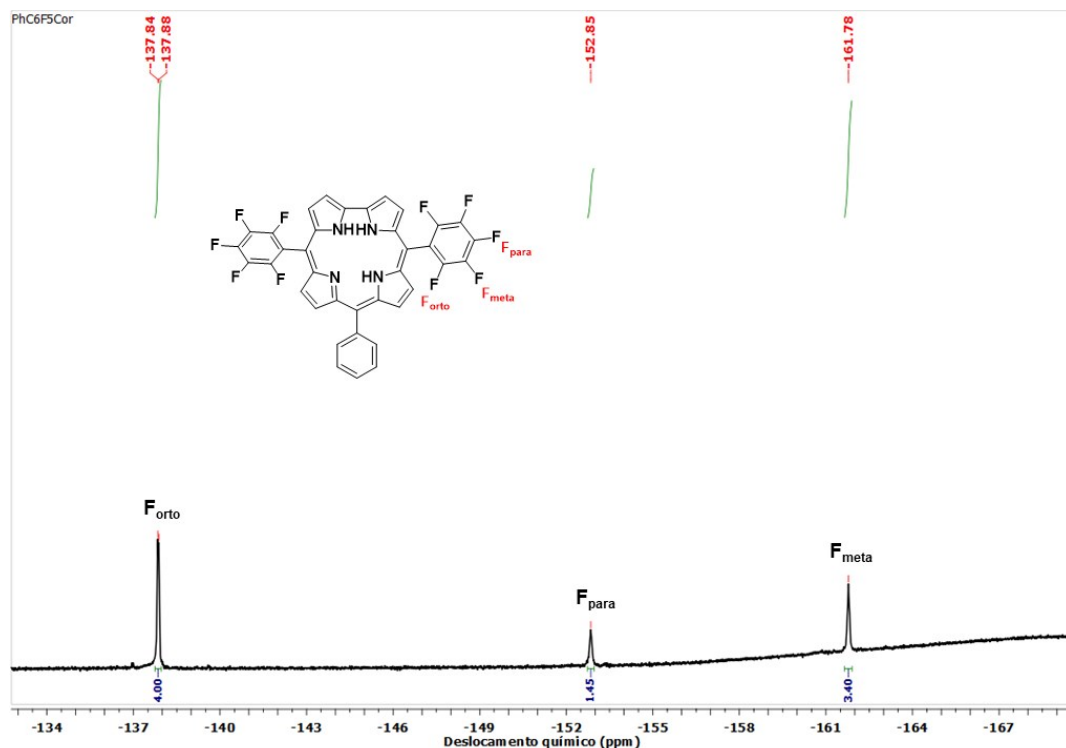


**Figure S7.**  $^{19}\text{F}$ -NMR spectra of corrole **1a**, in  $\text{CDCl}_3$ .

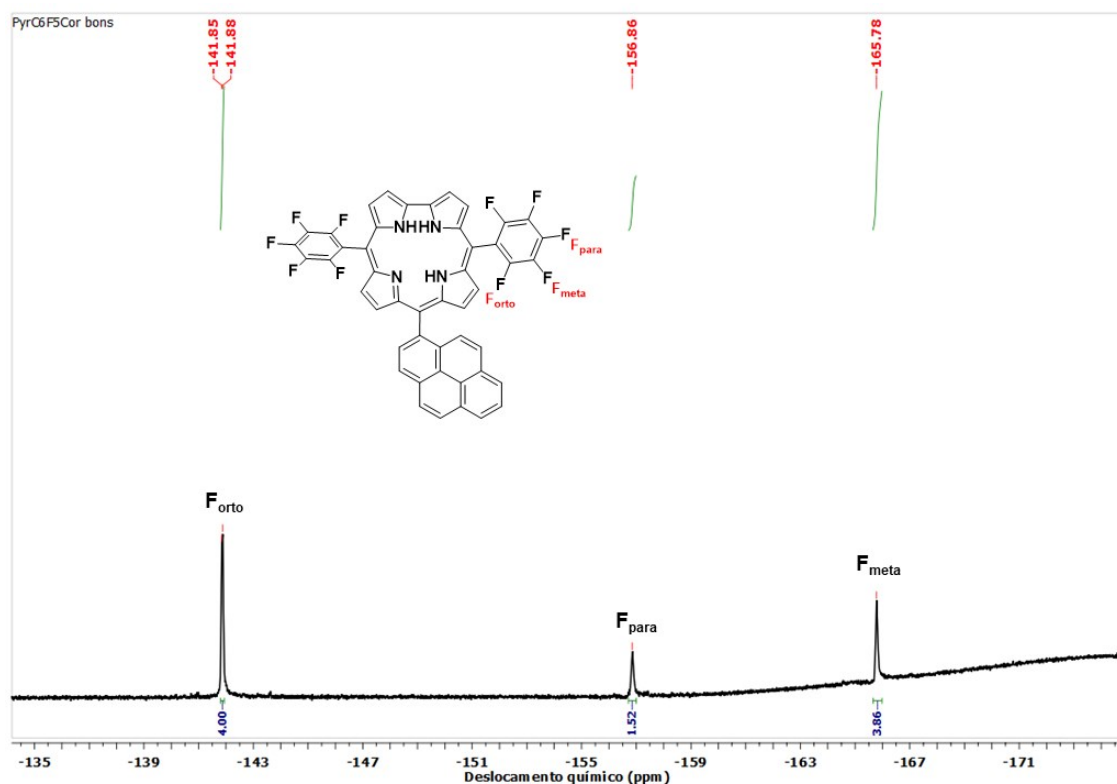


**Figure S8.**  $^{19}\text{F}$ -NMR spectra of corrole **1b**, in  $\text{CDCl}_3$ .

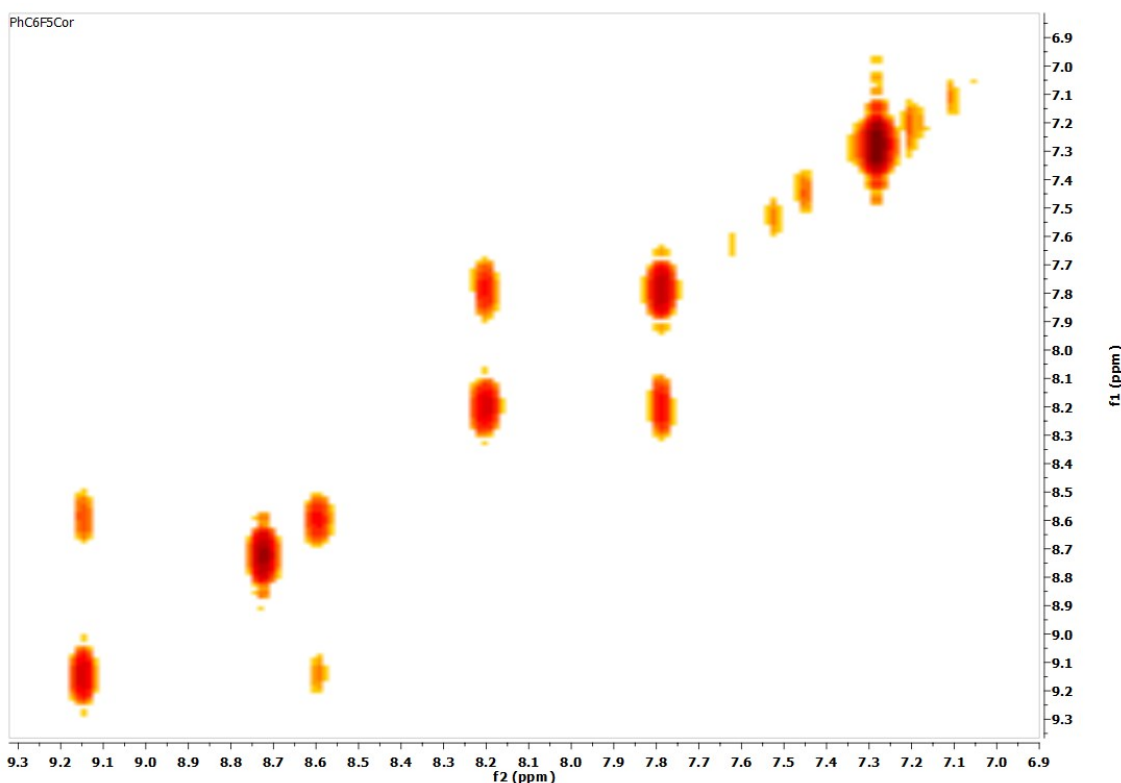


**Figure S9.** COSY 2D-NMR spectra of corrole **1a**, in  $\text{CDCl}_3$ .

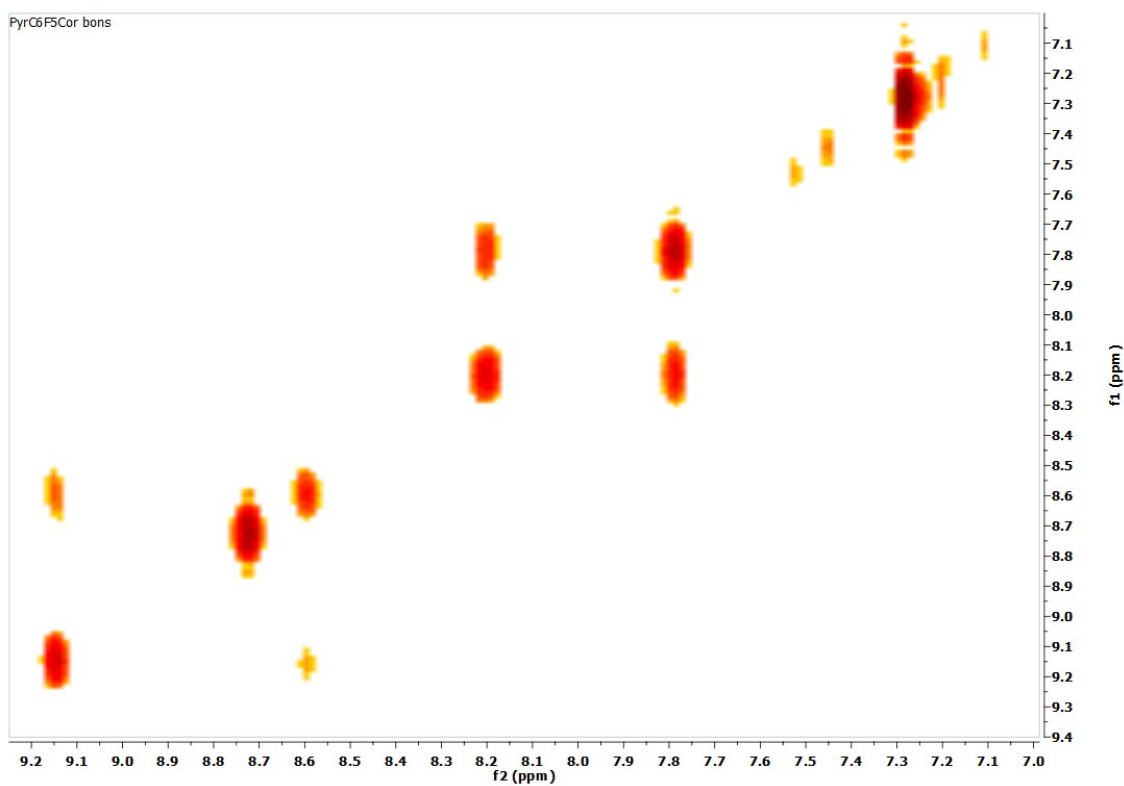


**Figure S10.** COSY 2D-NMR spectra of corrole **1a**, in  $\text{CDCl}_3$ .

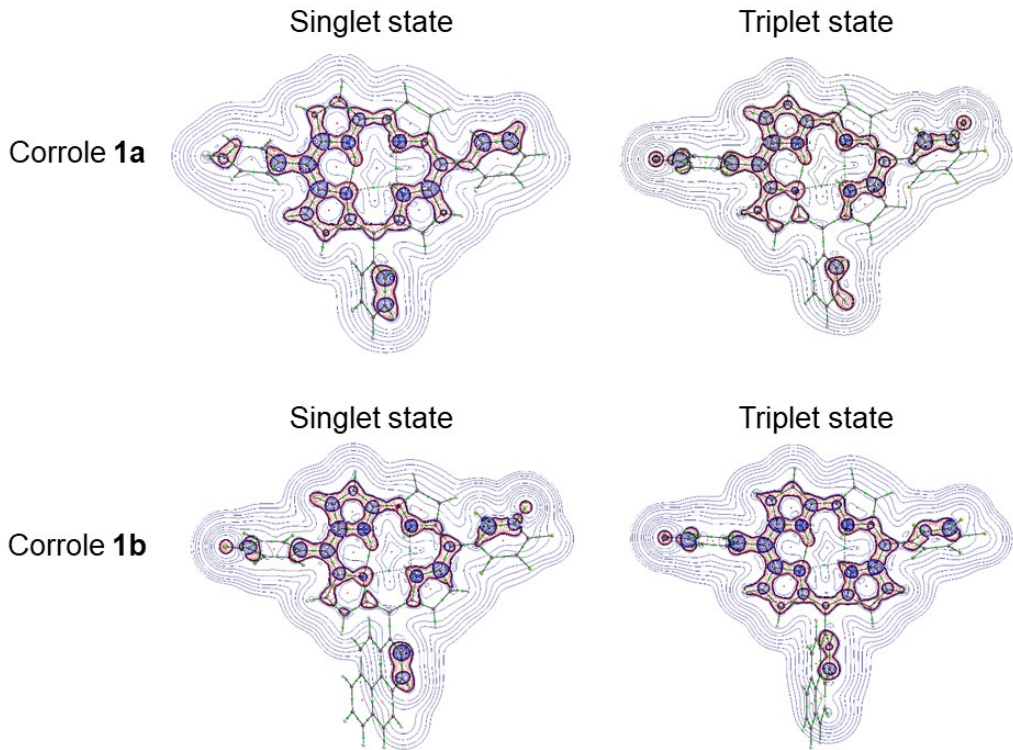


**Figure S11.** Laplacian of rho,  $\nabla^2(\rho)$ , of corroles **1a** and **1b**. On left top corner, the Triplet ( ${}^3S_0$ ) state followed by the Singlet ( ${}^1S_0$ ) of corrole **1a**, at right top corner; below, the same for corrole **1b**. The blue and red curves are quite similar.

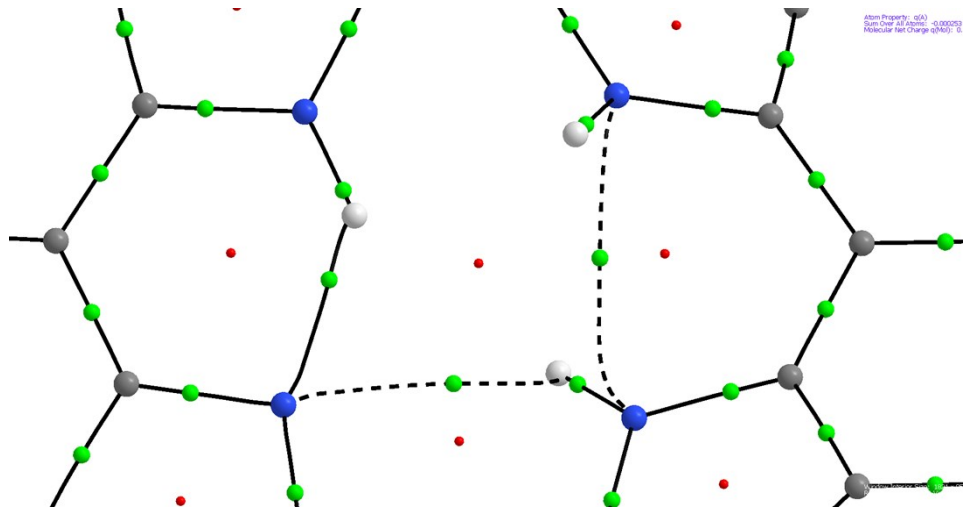


**Figure S12.** BCP map around the corrole center. It is possible to see that N16 interacts with both hydrogens, H35 and H37.

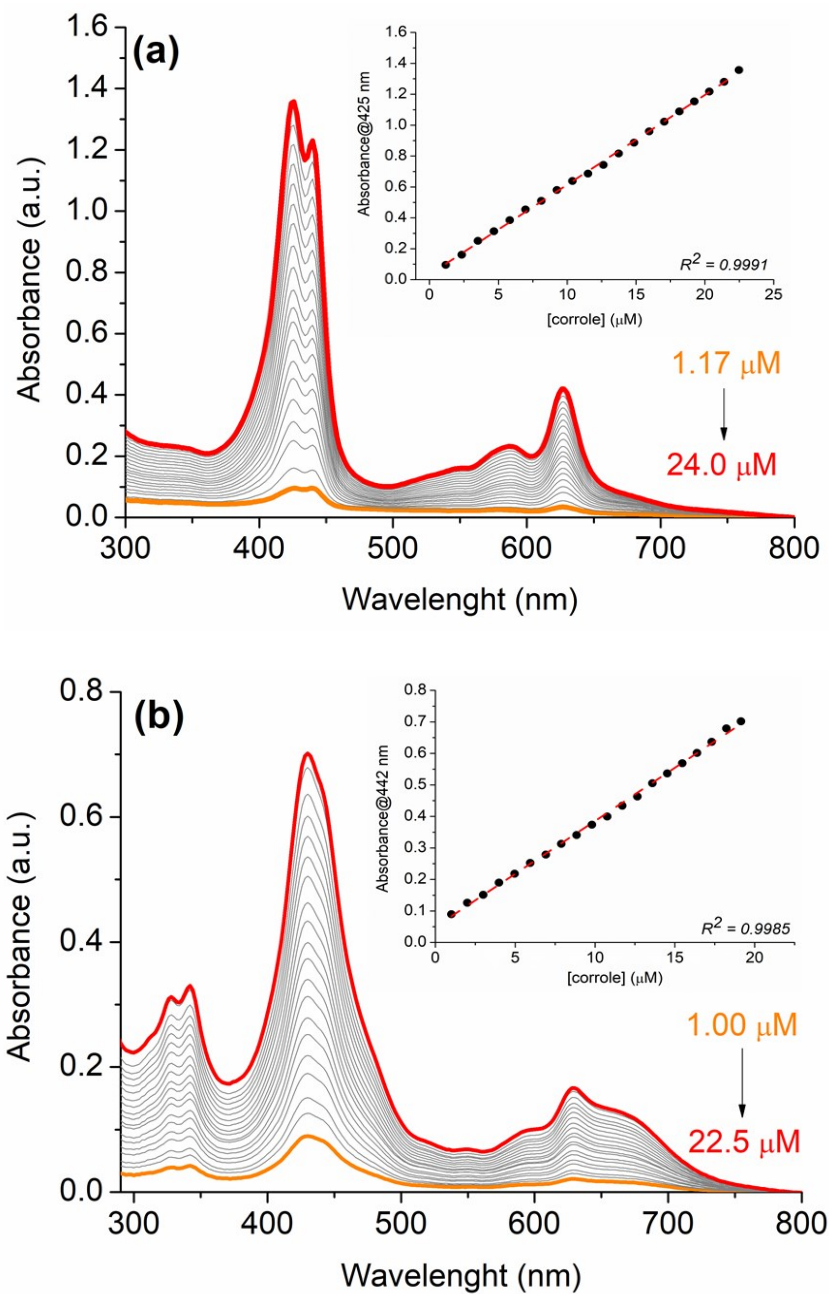


**Figure S13.** Aggregation study for **(a)** corrole **1a** and **(b)** corrole **1b**, using dimethyl sulfoxide (DMSO) as solvent. The *inset* shows the linear behavior of the absorbance at Soret band as a function of the concentration.

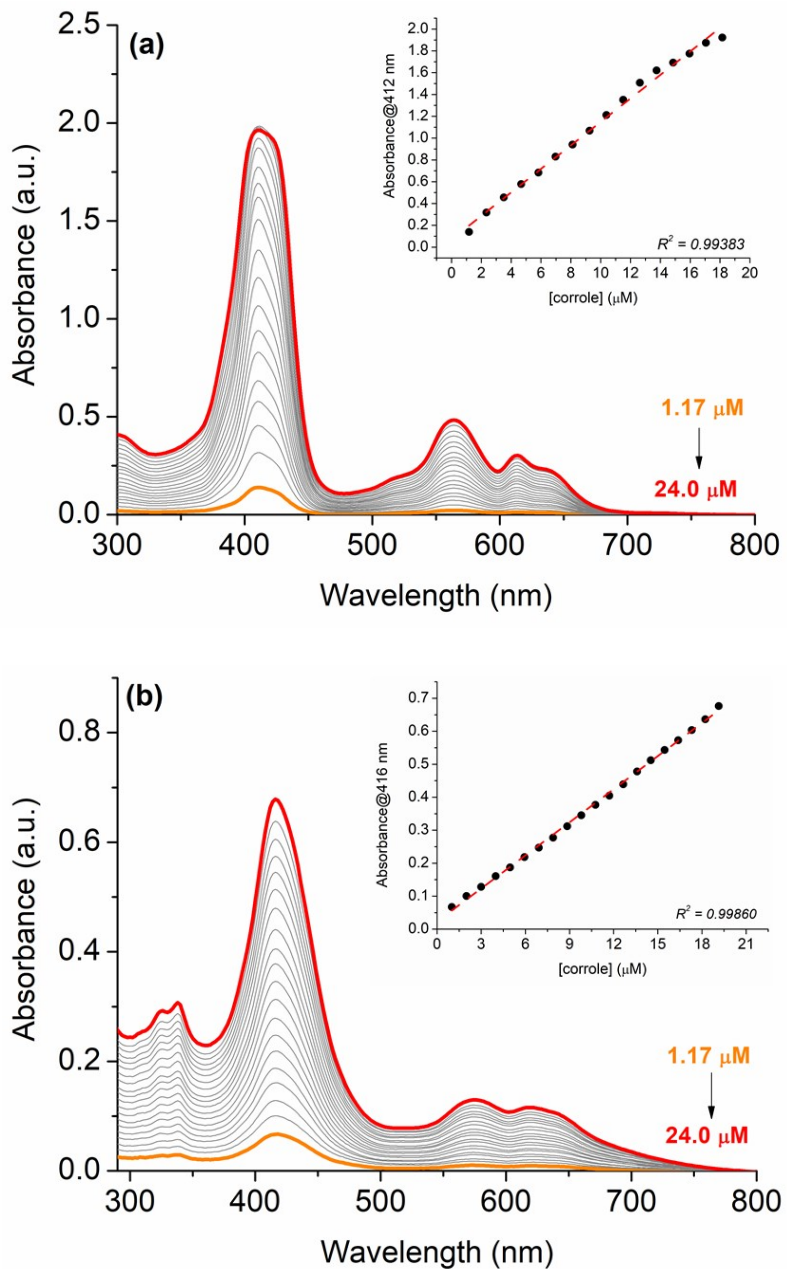


**Figure S14.** Aggregation study for **(a)** corrole **1a** and **(b)** corrole **1b**, using dimethyl sulfoxide (DCM) as solvent. The *inset* shows the linear behavior of the absorbance at Soret band as a function of the concentration.

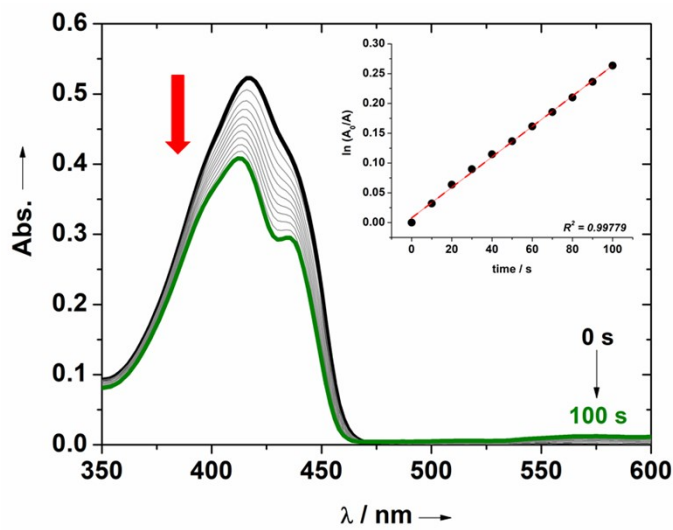


**Figure S15.** Photo-oxidation of DPBF by irradiation with diode laser (660 nm) in the presence of standard corrole **TPhCor**. The inset shows the kinetic profile.

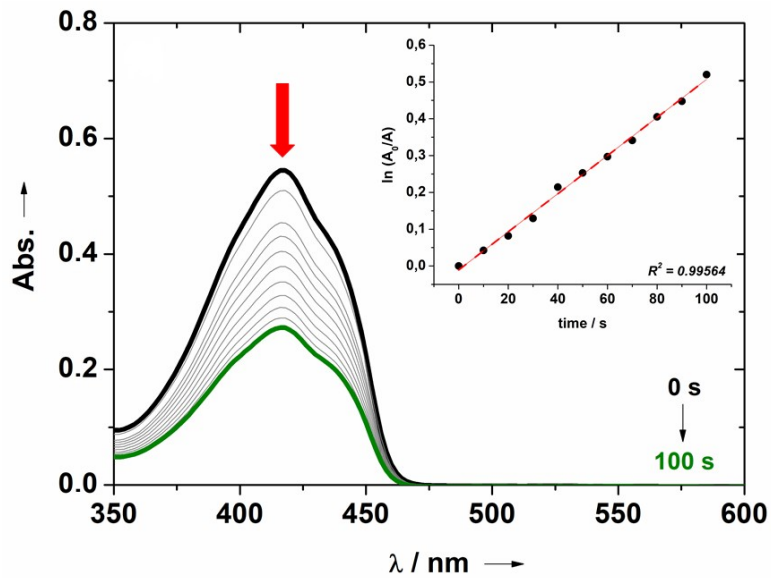


**Figure S16.** Photo-oxidation of DPBF by irradiation with diode laser (660 nm) in the presence of corrole **1a**. The inset shows the kinetic profile.

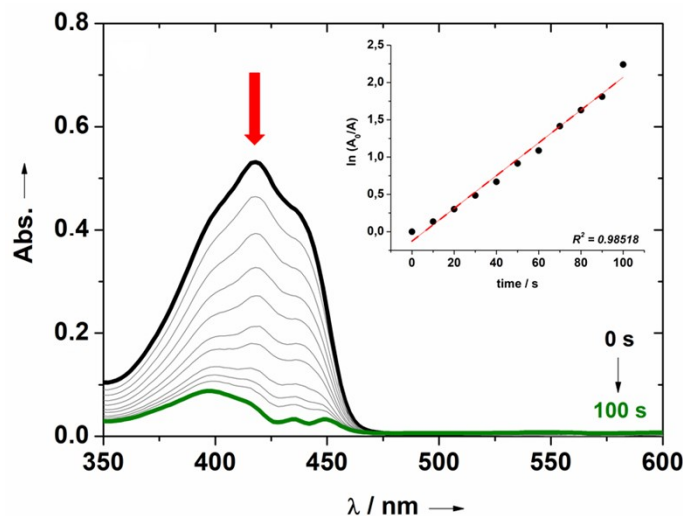


**Figure S17.** Photo-oxidation of DPBF by irradiation with diode laser (660 nm) in the presence of corrole **1b**. The inset shows the kinetic profile.

---

<sup>1</sup> D.T. Gryko, K. Jadach, A Simple and Versatile One-Pot Synthesis of meso-Substituted trans-A<sub>2</sub>B-Corroles, *J. Org. Chem.* 66 (2001) 4267-4275.

<sup>2</sup> P. Yadav, T. Anand, S.S.B. Moram, S. Bhattacharya, M. Sankar, S.V. Rao, Synthesis and femtosecond third order nonlinear optical properties of push-pull trans-A<sub>2</sub>B-corroles, *Dyes Pig.* 143 (2017) 324-330.